

RF VECTOR MEASUREMENT TEST-BENCH FOR EVALUATION OF BEHAVIORAL MODEL ACCURACY UNDER REALISTIC EXCITATION*

Maciej Myslinski¹, Kate A. Remley², Dominique Schreurs¹, Bart Nauwelaers¹

¹K.U.Leuven, Div. ESAT-TELEMIC, Kasteelpark Arenberg 10, B-3001 Leuven, Belgium
e-mail: maciej.myslinski@esat.kuleuven.be; phone: +32-16-321117; fax: +32-16-321986

²National Institute of Standards and Technology, Electromagnetics Division, 325 Broadway;
Boulder, CO 80305, USA
e-mail: remley@boulder.nist.gov; phone: +1-303-497-3652, fax: +1-303-497-3970

Abstract – This paper presents a simple test bench providing RF vector measurements of typical wireless communication system building blocks under realistic signal conditions. The instruments are synchronized by use of an experimental method based on an estimate of the signal path's time delay. As an example, a complex digitally modulated signal with a carrier frequency of 2.45 GHz was used. The ultimate goal of this test-bench is to deliver accurate measurement data enabling evaluation of the quality of large-signal behavioral models of the measured RF blocks.

Introduction

Large-signal behavioral modeling has been successfully applied to determine the behavior of various RF devices, components and circuits for modern wireless communication systems [1]. In the time-series modeling technique, the model is constructed based on the amplitude and phase of all spectral components of the incident and scattered traveling voltage waves of the device under test (DUT) as measured by a nonlinear vector network analyzer (NVNA) [2]. In previous studies, we showed that the experiment design, and in particular the type of excitation used during the measurements, determine the accuracy and the operational range of the resulting behavioral model [3]. In this perspective replacing single- or two-tone large-signal network analyzer (LSNA) measurements with a specific band-pass multisine counterpart led to both more efficient experiment design, and improved accuracy of the behavioral model in the operational range typical for wireless communication applications [4]. The increased accuracy results from the fact that we extract the model from the band-pass multisine designed to approximate realistic complex digitally modulated signals present in modern telecommunication standards [5].

In order to evaluate the quality of the proposed modeling method, we usually compare simulation and LSNA measurement results. We apply the waveform, as measured at the input of the DUT, as the excitation for the simulations. Up to now, we only used single-tone, two-tone, and multisine excitations. However, more credible evaluation of the LSNA measurement-based behavioral model's quality could be obtained through tests under realistic complex modulated signals typical for its final application. Unfortunately, these experiments cannot be performed in the LSNA set-up, due mainly to the existing limitation of the analyzer to work only with periodic signals and with relatively narrow modulation bandwidth [2]. Use of a simple spectrum analyzer should not be considered because in this case it provides information on only the magnitude, whereas the phase information is missing. This is not a

* Work partially supported by the U.S. government, not subject to copyright in the United States.

satisfying solution, especially when a significant part of the information carried by the signal resides in its phase. Therefore, we would rather use a vector signal analyzer or an equivalent instrument that provides full knowledge of both amplitude and phase of the complex digitally modulated signal.

In the following sections of this work, we describe an RF vector measurement test bench designed to test RF amplifiers under realistic complex modulated excitations. We propose an experimental method to synchronize the instruments in the set-up in order to correctly acquire measurement data. The procedure is illustrated by an example of a code division multiple access (CDMA) quadrature phase shift keying (QPSK) signal with 1.6 MHz bandwidth generated at two carrier frequencies in the 2 GHz and 5 GHz range.

Measurement set-up description

The proposed measurement set-up is based on two instruments: the vector signal generator (VSG) and the vector signal analyzer (VSA), as presented in Fig. 1. The VSG stores in its memory the in-phase, $I(t)$, and quadrature, $Q(t)$, components of the modulated-signal waveform calculated by commercial design-environment software. The VSG then upconverts these waveform components to a given carrier frequency and generates them at a given power level. On the opposite side of the signal path we locate the VSA. This instrument, when properly adjusted and synchronized with the rest of the measurement set-up, provides time- and frequency-domain vector measurement of the signals at the output of an RF amplifier.

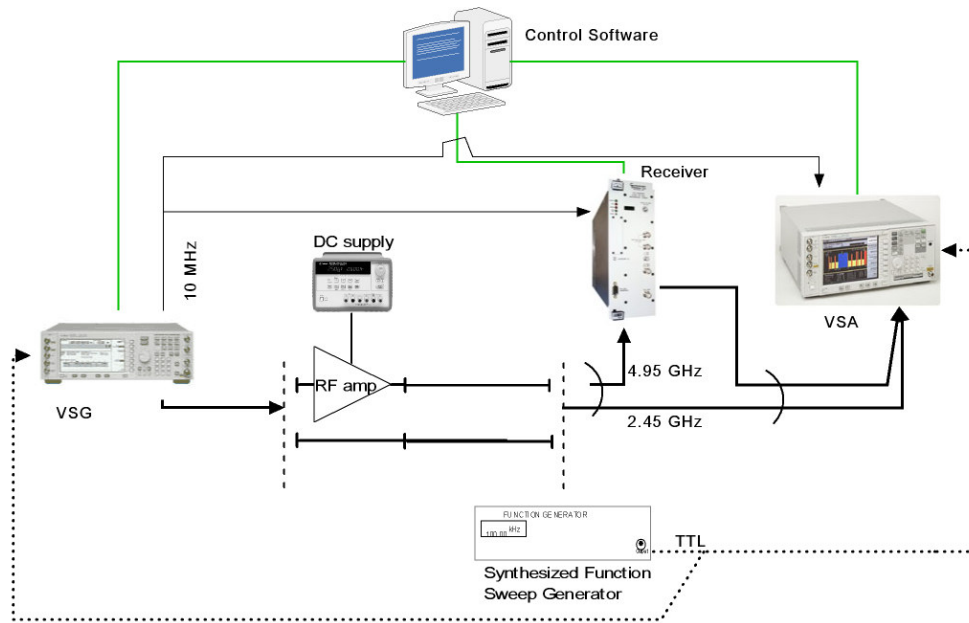


Fig. 1. Schematic of the RF vector measurement set-up.

Apart from the RF amplifier measurements, we also perform measurements of the full cable path from VSG to VSA, with the nonlinear circuit replaced by an adapter. Finally, the direct connection between the generator and the analyzer is realized in order to obtain measurements of the signal exciting the RF amplifier under test. This step is particularly important since we desire to apply such measurement results as the excitation during the simulation of investigated behavioral models. In fact, what we need is to test the model under exactly the same excitation as used in the measurements. In this perspective, the ability to emulate the signal in the simulation environment is not enough. This calculated waveform will differ from the signal at the DUT input, due to the nonideal signal generation process in the VSG. Amplitude and phase distortions, IQ balance impairments, and spectral regrowth will become more pronounced with increasing output power. Some manufacturers offer a software/hardware solution to

overcome these generator-related problems. An alternative approach to counteract the nonideality of the generation process, but focused more on signal statistics, has been presented in [6]. In our case, we measure the VSG output with the VSA and use this measured result as the excitation during the model testing. The connectivity between the VSA and the CAD software is relatively easy to make through a standard component from the simulator's library.

As shown in Fig. 1, the VSG's internal 10 MHz oscillator is used as the reference signal in the set-up, whereas the synthesized function/sweep generator provides triggering events for both VSG and VSA. The detailed discussion of the instrument synchronization will be given in the next section. The last instrument included in the schematic of Fig.1 is a tunable, broadband RF receiver that converts signals above 2.7 GHz (the upper frequency limit of the VSA) down to 1 GHz.

Obviously, correct set up of the instruments is no less important than the instruments themselves for credible and accurate measurements. First of all, we should set the appropriate VSA input range by switching the built-in attenuators. Setting the VSA's input range too low with respect to the input signal level (more sensitive than necessary) causes the analyzer's analog-to-digital circuit (ADC) to introduce distortion into the measurement. On the other hand, setting the VSA's input range much higher than the power level of the incoming signal (less sensitive than necessary) may cause a loss of dynamic range due to additional noise. In some cases, the increase in the noise floor may even obscure low-level frequency components [7, 8].

Subsequently, VSA time- and frequency-domain parameters should be adjusted according to the applied signal. We start with an acquisition data block size large enough to acquire at least the entire waveform generated by the VSG. At the same time, we adjust the frequency span to match the clock of the I/Q modulator of the VSG. In general, this sampling frequency should be at least three to four times the bandwidth of a signal in order to observe intermodulation distortion introduced by the RF amplifier measured. However, we observed that increasing the sampling frequency by more than four times the signal's bandwidth improves the delay estimation and improves the smoothness of the measured waveforms. Finally, we should note that both the sampling frequency and the acquisition data block length determine the resolution bandwidth of the VSA measurement. In the case we considered of a CDMA-QPSK signal having a 1.2288 MHz bandwidth, we measured one full block of 65536 data samples generated with the sampling frequency eight times the signal's bandwidth. The resulting resolution bandwidth is 150 Hz. Note that many of the VSA parameters are related to each other and cannot be independently set to any value. For example, the time-record length is limited by the frequency span and number of frequency points.

Trigger synchronization

The RF measurement test bench of Fig. 1 is composed of at least two instruments requiring both trigger synchronization and measurement data acquisition at a specific time and sequence. This is common in RF measurement systems for telecommunication applications [9]. The signal waveform stored in the VSG's memory after upconversion, transmission, downconversion and detection should be completely acquired by the VSA. A difficulty in this case is that the acquired signal occupies a full data block in the VSA's memory. Thus, any error in the generation-acquisition synchronization could lead to loss of data samples, sampling in wrong timestamps, or in general poor repeatability of the measurements.

The synchronization method of the instruments in the configuration shown in Fig.1 requires an external function generator providing the necessary triggering signal. For this purpose we use a synthesized function/sweep generator operating at 1 Hz and delivering a TTL signal to trigger both the VSA and the VSG. Fig. 2 depicts the first 20 microseconds of the $I(t)$ and $Q(t)$ CDMA waveforms stored in the VSG (solid red line) and detected by the VSA (blue line with stars). The plotted waveforms are normalized in order to facilitate the comparison. Due to the large number of samples it is difficult to visually compare calculated and measured data. Therefore we plot only the first 20 microseconds of the waveforms considered.

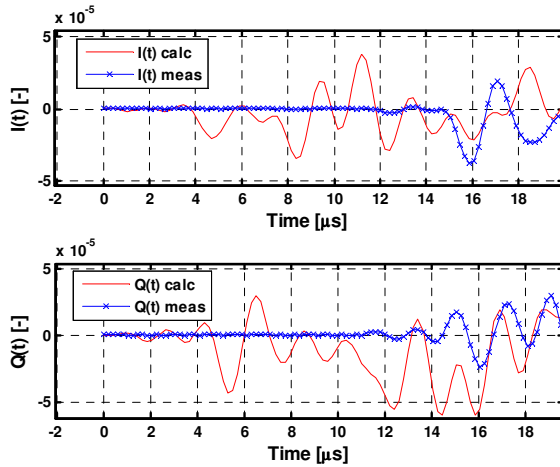


Fig. 2. The first 20 microseconds of the $I(t)$ and $Q(t)$ CDMA waveforms.

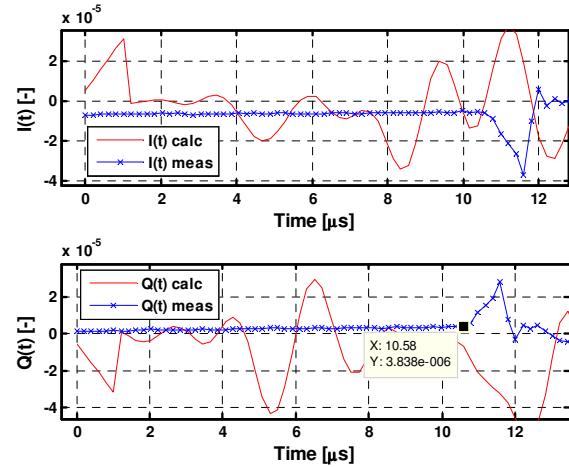


Fig. 3. The first 12 microseconds of the modified $I(t)$ and $Q(t)$ CDMA waveforms – used in the delay estimation.

As we can see, the measured waveforms are delayed by approximately 10 microseconds with respect to their calculated counterparts. This delay accumulates along the signal path from the baseband generator, through the I/Q modulator, the digital filters and other signal conditioning blocks of the VSG front end, down through the cable, the attenuators, demodulator, and ADC in the VSA. Note that the delay was also present when we used data markers in the generated waveform instead of the external function generator to trigger VSA. The delay leads to incomplete acquisition of the I/Q waveforms due to the fact that the data acquisition block has the same length as the generated I/Q data and the sampling frequencies of both instruments are also the same. Therefore, we need to account for this delay during the synchronization of the instruments.

Trigger delay estimation

A straightforward solution to synchronize signal generation and acquisition is to delay the trigger of the VSA by the same interval as the observed delay in the signal path. However, from Fig. 2 it is very difficult to accurately estimate the delay value because the amplitudes of the first data samples are very small.

We propose an experimental method to accurately estimate the signal path delay. For this purpose we perform initial measurements using modified $I(t)$ and $Q(t)$ waveforms. We change the values of the first six $I(t)$ and $Q(t)$ data samples to obtain a visible difference between the null signal and the actual start of the incoming data samples. This modification has a ramp-like shape with linearly increasing values in the case of $I(t)$, and decreasing in the case of $Q(t)$. After generation and detection, the measured $I(t)$ and $Q(t)$ waveforms can be compared with the corresponding modified calculated waveforms, as presented in Fig. 3. We obtain the value of the delay as the time of the sixth sample before the peak in the introduced ramp. In the example shown here for a CDMA-QPSK signal at 2.45 GHz, the delay is equal to 10.58 microseconds. In terms of sampled time vector, it occurs at the 53rd time sample.

When the VSA is triggered with the experimentally found delay, we obtain the $I(t)$ and $Q(t)$ waveforms as shown in Fig.4. Both the calculated and measured waveforms are well aligned in time; however, for some time intervals, a 180° shift is observed. We noticed that in most cases the measured $I(t)$ and $Q(t)$ waveforms are swapped and inverted with respect to the original calculated data. The observed $I(t)$ and $Q(t)$ swapping is similar to multiplying a complex number by minus the imaginary unit ($-j$). Therefore a possible cause of this effect might be related to the Hilbert transformation of the signal performed somewhere in the software or hardware parts of the measurement set-up.

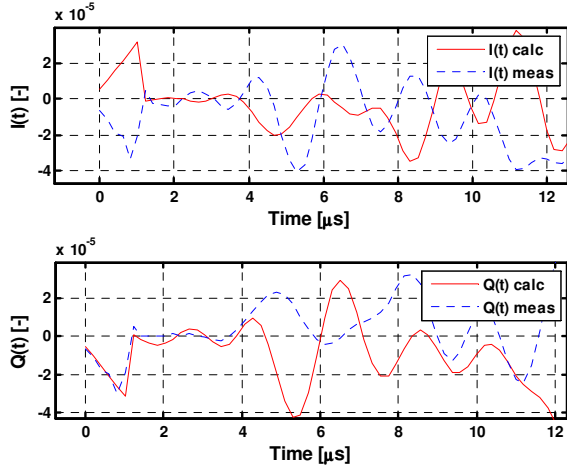


Fig. 4. The first 12 microseconds of the modified I(t) and Q(t) CDMA waveforms measured with VSA triggered with the experimentally found delay.

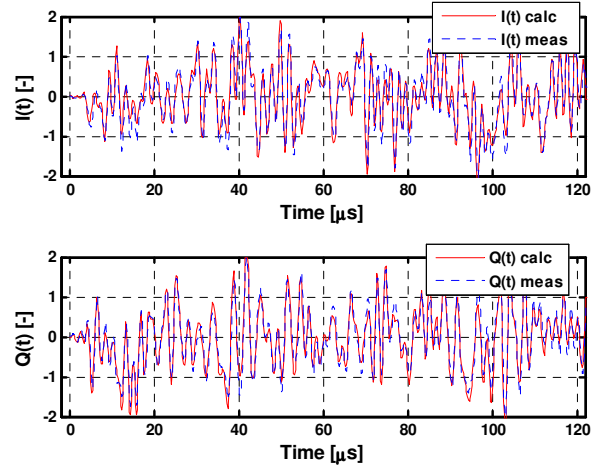


Fig. 5. The first 120 microseconds of the I(t) and Q(t) CDMA waveforms with swapped measured I(t) and Q(t) waves according to (3).

If we write the complex envelopes downloaded to the VSG and detected by the VSA in terms of their real and imaginary parts, we obtain

$$Z_G(t) = I_G(t) + jQ_G(t), \text{ and } Z_D(t) = I_D(t) + jQ_D(t), \text{ respectively.} \quad (1)$$

We can express the detected complex envelope $Z_D(t)$ as a product of minus the imaginary unit and the complex envelope $Z_G(t)$ downloaded to the VSG:

$$Z_D(t) = -jZ_G(t) = -jI_G(t) + Q_G(t). \quad (2)$$

Then, from (1) and (2), we get the following transformation of I(t) and Q(t) waveforms:

$$\begin{cases} I_D(t) = Q_G(t) \\ Q_D(t) = -I_G(t). \end{cases} \quad (3)$$

Fig.5 illustrates how transformations (3) improved the match between measured and calculated I(t) and Q(t) waveforms. The measured I(t) and Q(t) waveforms now closely correspond to calculated waveforms stored in the VSG memory. We should mention that the delay remained almost unchanged when we performed the tests on different carrier frequencies.

Conclusion

In this work we described the RF vector measurement test-bench designed for testing RF components under realistic complex modulated signals. We discussed the most important settings of the instruments that are indispensable for proper data acquisition. Finally, we presented a method of trigger synchronization based on the experimental estimation of the time delay in the signal path. As a result, we obtained a very good match between the measured and the calculated I(t) and Q(t) waveforms demonstrated for the case of a CDMA-QPSK signal having a 1.6 MHz bandwidth, generated and measured at 2.45 GHz. The presented set-up can be used to verify, in a realistic signal environment, the accuracy of LSNA measurement-based behavioral models of RF components for wireless telecommunication systems.

Acknowledgement

Maciej Myslinski is the recipient of an ARFTG Fellowship, which partially supported this work along with NIST and the FWO project G.0405.03. Dominique Schreurs is supported by the Fund for Scientific Research-Flanders as a postdoctoral fellow.

References

- [1] J. Wood and D.E. Root, "Fundamentals of Nonlinear Behavioral Modeling for RF and Microwave Design", *Artech House*, 2005.
- [2] J. Verspecht, P. Debie, A. Barel, and L. Martens, "Accurate on wafer measurements of phase and amplitude of the spectral components of incident and scattered voltage waves at the signal ports of a nonlinear microwave device," *IEEE Digest of International Microwave Symposium (MTT-S)*, Orlando, USA, pp. 1029-1032, 16-20 May 1995.
- [3] D. Schreurs, M. Myslinski, and K.A. Remley, "RF behavioural modelling from multisine measurements: influence of excitation type", *European Microwave Conference (EuMW)*, Munich, Germany, pp. 1011-1014, 7-9 October 2003.
- [4] M. Myslinski, D. Schreurs, K.A. Remley, M.D. McKinley and B. Nauwelaers, "Large-Signal Behavioral Model of a Packaged RF Amplifier Based on QPSK-Like Multisine Measurements", *Proc. Gallium Arsenide and other Compound Semiconductors Application Symposium (GAAS)*, Paris, France, pp. 185-188, 3-4 October 2005.
- [5] J.C. Pedro and N.B. Carvalho, "Designing multisine excitations for nonlinear model testing", *IEEE Transactions on Microwave Theory and Techniques*, Vol. 53, No. 1, pp. 45-54, Jan. 2005.
- [6] N. B. Carvalho and J. C. Pedro, "Laboratory Generation of Multi-Sines with Pre-described Statistics", *Proc. 35th European Microwave Conference (EuMW)*, Paris, France, pp. 1199-1202, October 2005.
- [7] VSA documentation available on-line at <http://www.home.agilent.com/USeng/nav/-536902949.0/pc.html>.
- [8] M.D. McKinley, K.A. Remley, M. Myslinski, J.S. Kenney, "Eliminating FFT artifacts in vector signal analyzer spectra," *to be published in Microwave Journal*, Oct., 2006.
- [9] Materials available on-line at <http://www.keithley.com>.